PNAS
www.pnas.org

Supplementary Information for:

Disentangling the role of photosynthesis and stomatal conductance on rising forest water-use efficiency

Rossella Guerrieri[a,b,1], Soumaya Belmecheri[c], Scott V. Ollinger[a], Heidi Asbjornsen[a], Katie Jennings[a], Jingfeng Xiao[a], Benjamin D. Stocker[b], Mary Martin[a], David Y. Hollinger[d], Rosvel Bracho-Garrillo[e], Kenneth Clark[f], Sabina Dore[g], Thomas Kolb[g], J. William Munger[h], Kimberly Novick[i], and Andrew D. Richardson[j,k]

[a]Earth Systems Research Center, University of New Hampshire, Durham, NH 03824; [b]Centre for Ecological Research and Forestry Applications, c/o Universidad Autonoma de Barcelona, 08290 Cerdanyola, Barcelona, Spain; [c]Laboratory of Tree-Ring Research, University of Arizona, Tucson, AZ 85721; [d]Northern Research Station, US Department of Agriculture Forest Service, Durham, Q:7 NH 03824; [e]School of Forest Resources and Conservation, University of Florida, Gainesville, FL 32611; [f]Silas Little Experimental Forest, Northern Research Station, US Department of Agriculture Forest Service, New Lisbon, NJ 08064; [g]School of Forestry, Northern Arizona University, Flagstaff, AZ 86011; [h]School of Engineering and Applied Sciences, Harvard University, Cambridge, MA 02138; [i]School of Public and Environmental Affairs, Indiana University, Bloomington, IN 47405; [j]Center for Ecosystem Science and Society, Northern Arizona University, Flagstaff, AZ 86011; [k]School of Informatics, Computing and Cyber Systems, Northern Arizona University, Flagstaff, AZ 86011

[1]Corresponding author:
Rossella Guerrieri
Email: rossellaguerrieri@gmail.com

This PDF file includes:

Supplementary text
Figures S1 to S19
Tables S1 to S8
SI reference citations

www.pnas.org/cgi/doi/10.1073/pnas.1905912116

Supplementary Text

Meta-analysis of studies in the US reporting $\delta^{13}C$ and $\delta^{18}O$ values in tree-rings

Dendro-isotopic studies from the U.S. were found from an online literature search that was conducted from January to May of 2016 on the ISI Web of Science using search terms including 'stable isotopes', 'tree rings', 'US' & 'USA'. Studies were included in the meta-analysis if they presented data on stable carbon or oxygen isotopes from tree rings sampled from trees that were not part of a manipulative experiment. Coordinates for each study site were collected or estimated using site names and other specific information from the publication in order to create a broad-scale map showing the spatial distribution of dendroisotopic studies across the U.S. (Figure S1).

Modeling $\delta^{18}O$ of precipitation and $\delta^{18}O$ at the evaporative site

We estimated annual values of precipitation $\delta^{18}O$ ($\delta^{18}O_P$) at each site by considering the following equation [1]:

$$\delta^{18}O_P = 0.52T_a - 0.006T_a^2 + 2.42P_a - 1.43P_a^2 - 0.046\sqrt{E} - 13.0 \qquad \text{(S1)}$$

where T_a, P_a and E are the annual temperature, precipitation (this latter expressed in m) and elevation (m *asl*), respectively. The obtained values were used in the equation 4 to calculate the $\Delta^{18}O_c$, which was used to estimate the leaf water $\Delta^{18}O$ ($\Delta^{18}O_{LW}$) as described in the main text. Moreover, $\delta^{18}O$ was also used to estimate the ^{18}O enrichment at the evaporative site above the source water ($\Delta^{18}O_e$). The evaporative enrichment model of a free water surface [2] is commonly applied to predict the $\Delta^{18}O_e$ [3,4], which is described by the following equation:

$$\Delta^{18}O_e = \varepsilon^+ + \varepsilon_k + (\Delta^{18}O_v - \varepsilon_k)\,\frac{e_a}{e_i} \qquad \text{(S2)}$$

ε_k is the kinetic fractionation during diffusion through the stomata and leaf boundary layer, ε+ the proportional depression of water vapor pressure by the heavier $H_2{}^{18}O$ molecule, $\Delta^{18}O_v$ is the $\delta^{18}O$ of water vapor relative to source water and, finally, e_a/e_i is the ratio of ambient to intercellular water vapor mole fraction. The fractionation factors ε_k and ε+ can be calculated by using the following equations [4,5,6]:

$$\varepsilon^+ = \left[\exp\left(\frac{1.137}{(273+T)^2}\cdot 10^3 - \frac{0.4156}{273+T} - 2.0667\cdot 10^{-3}\right) - 1\right]\cdot 1000 \qquad \text{(S3)}$$

$$\varepsilon_k = \frac{32r_s+21r_b}{r_s+r_b}/1000 \qquad \text{(S4)}$$

where T is the leaf temperature in °C, and r_s and r_b are the stomatal and boundary layer resistances, respectively, which are the inverses of the stomatal (g_s) and boundary layer (g_b) conductances. The number 32 and 21 are the fractionation factors (expressed in ‰) for diffusion through air and boundary layer [3]. Assuming that the water vapor in the air is in isotopic equilibrium with source water, then $\Delta^{18}O_v$ will approximately equal ε^+ [6] so that the equation S2 will become:

$$\Delta^{18}O_e = \varepsilon^{+} + \varepsilon_k \cdot (1 - \frac{e_a}{e_i}) \quad \text{(S5)}$$

We derived the $\Delta^{18}O_e$ for two years and at two sites where $\delta^{18}O$ in leaf, stem and soil water was measured (see below). For calculating ε_k, we assume g_b = 1 mol m^{-2} s^{-1} [7], while we considered values shown in [8] for g_s: 0.09 mol m^{-2} s^{-1} for the pine trees at Austin Cary and the average between g_s for deciduous (0.17 mol m^{-2} s^{-1}) and conifers (0.09 mol m^{-2} s^{-1}) for the oak and hemlock trees at Harvard forest. Assuming leaf temperature to be similar to air temperature, e_a/e_i is equal to relative humidity [6].

We compared our estimates of $\delta^{18}O_P$ (here source water), $\Delta^{18}O_{LW}$ (estimated as described in the Methods) and $\Delta^{18}O_e$ with measured values of $\delta^{18}O$ in soil/stem water and $\Delta^{18}O_{LW}$ for two consecutive years (2005 and 2006) at two of the eight investigated sites, i.e., Harvard and Austin Cary forests [9]. The two sites are representative of the two contrasting moisture conditions (the mesic Harvard forest in the Northeastern U.S. and xeric forest at Austin Cary in the Southeastern U.S.). Data derived from measurements carried out on 3-4 days during summer 2004 and 2005 between 12 pm and 3 pm. Soil $\delta^{18}O$ was measured in the first 10 cm of the soil, while leaf water $\delta^{18}O$ was measured on leaves and needles sampled from n=two trees for *Quercus rubra* (Harvard forest) and *Pinus elliottii* (Austin Cary Memorial forest), respectively for each sampling day. $\Delta^{18}O_{LW}$ was calculated by considering measured $\delta^{18}O$ in soil/stem and leaf water according to equation 4 in the Methods (main text). Comparison between estimated $\Delta^{18}O_{LW}$ and $\Delta^{18}O_e$ *vs.* measured values are shown in the Figure S9. Our estimates of $\Delta^{18}O_{LW}$ are in the same order of magnitude or perform somehow better (i.e., they fall within the confidence interval of actual measurements) than those obtained from the Craig and Gordon model

[2] (for instance in the case of Austin Cary). This is likely due to the fact that $\Delta^{18}O_e$ depends on relative humidity. For the two consecutive years were comparison was carried out, relative humidity at the two sites had similar values (70 % at HF and 77% at ACMF), while growing season temperature was higher at ACMF (26 ºC) than HF (18 ºC). This difference in temperature is captured in our estimate, as we estimated the ε_{wc} based on growing season temperature (see Methods). Moreover, the other limitation of the Craig and Gordon model is that some of the assumptions may not be true at all the sites and for all the tree species considered (e.g., same g_s values for conifer and/or deciduous, no changes in g_s, same value for g_b across all species). Given that we did not observe significant changes in relative humidity for the majority of the sites (Figure S19), changes in $\Delta^{18}O_{LW}$ as obtained by our backward estimates from measured tree-ring alpha-cellulose $\delta^{18}O$ likely reflect a reduction in g_s, and hence transpiration, rather than changes in relative humidity [4].

Leaf area index trend

The Leaf Area Index (LAI) data from 2002 to 2012 were obtained from MODIS/Terra+Aqua Leaf Area Index (LAI) 8-Day for the eight sites included in the study and with 500 m pixel size [10]. Data were filtered to include only the following quality check conditions: 1- significant clouds NOT present (clear); 2- SCF quality control was "Main (RT) method used, best result possible (no saturation)" and/or "Main (RT) method used with saturation. Good, very usable". Further, we subset the data so to consider the growing season (grs) months (May-September) and then we calculated the average over the maximum value of LAI for each month. Data were retrieved from the online Application for Extracting and Exploring Analysis Ready Samples (AppEEARS), courtesy of the NASA EOSDIS Land Processes Distributed Active Archive Center (LP DAAC), USGS/Earth Resources Observation and Science (EROS) Center, Sioux Falls, South Dakota, available at the following link: https://lpdaacsvc.cr.usgs.gov/appeears/.

Figure S1 Overview of tree-ring isotopes studies in the U.S. Map reporting our sites and where previous tree ring isotope-related studies were carried out in the U.S. Circles indicate studies where both isotope ratios ($\delta^{13}C$ and $\delta^{18}O$) were measured (sites included in this study are indicated in red). Whereas green and blue triangles indicate studies were only $\delta^{13}C$ or $\delta^{18}O$ were measured, respectively. Note that previous studies looked at tree-ring isotopes at Harvard Forest [11,12] and Silas Little [13], though in this latter case only two years were considered. See the supplementary text for more details on the meta-analysis.

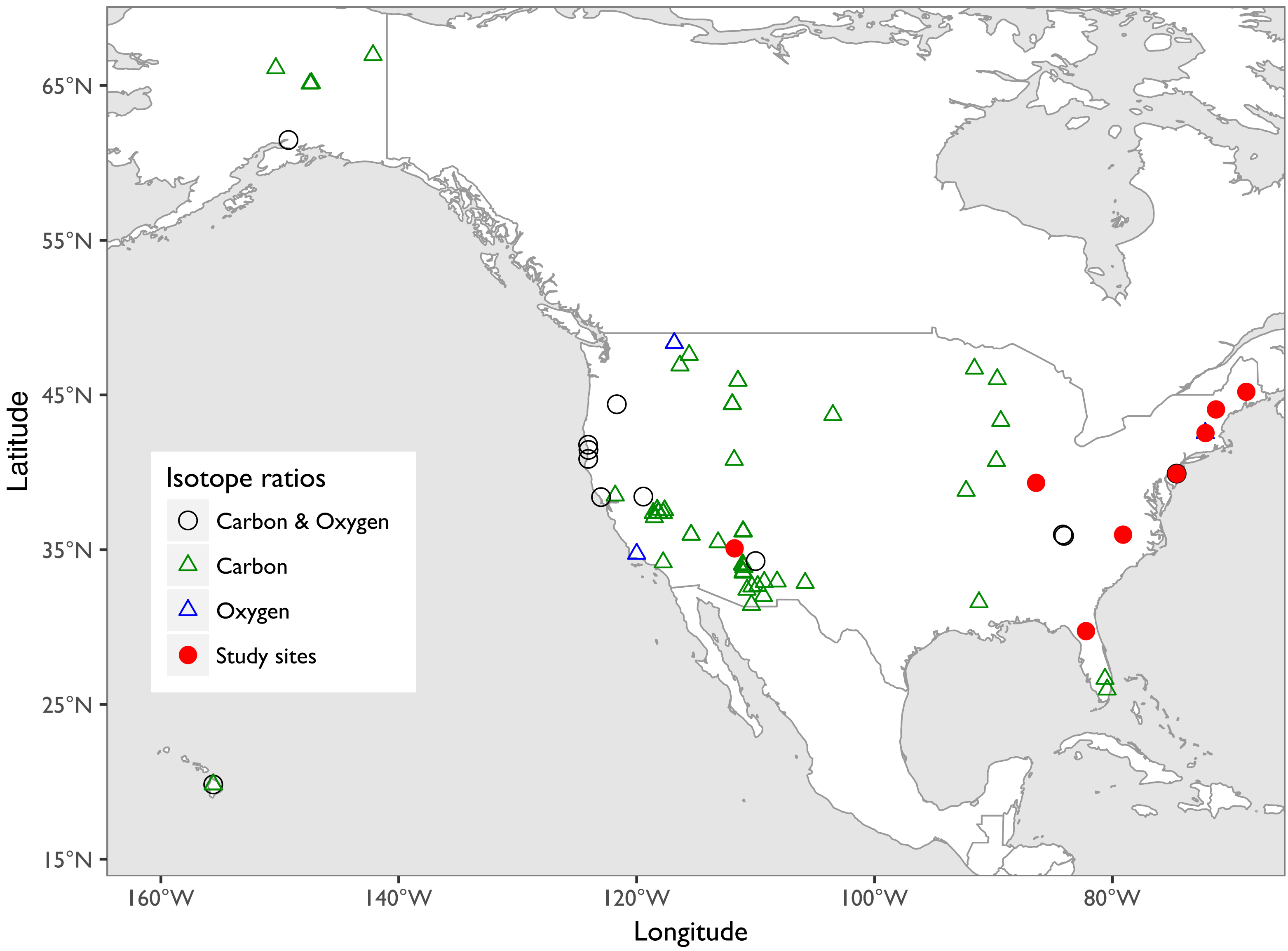

65°N
55°N
45°N
35°N
25°N
15°N
Latitude
160°W
140°W
120°W
100°W
80°W
Longitude
Isotope ratios
Carbon & Oxygen
Carbon
Oxygen
Study sites

Figure S2 Long-term changes in intrinsic water-use efficiency. Trends in intrinsic water-use efficiency (iWUE) for the 12 tree species at eight AmeriFlux sites. Each point represents the values obtained from alpha-cellulose $\delta^{13}C$ ($\delta^{13}C_c$) measured for the last 30 years from n=5 replicates per species at each of the investigated site (for a total of 75 chronologies). We observed an increase in iWUE for the majority of the species, with the exception of *Pinus echinata* (piec) at Silas Little, where iWUE decreased, and *Acer saccharum* (acsa) at Morgan Monroe and *Tsuga canadensis* (tsca) at Bartlett, where no significant changes were found. The full name of sites and species is provided in Table S1. Note that some species are present at more than one site (e.g., *Tsuga canadensis* and *Liriodendron tulipifera*).

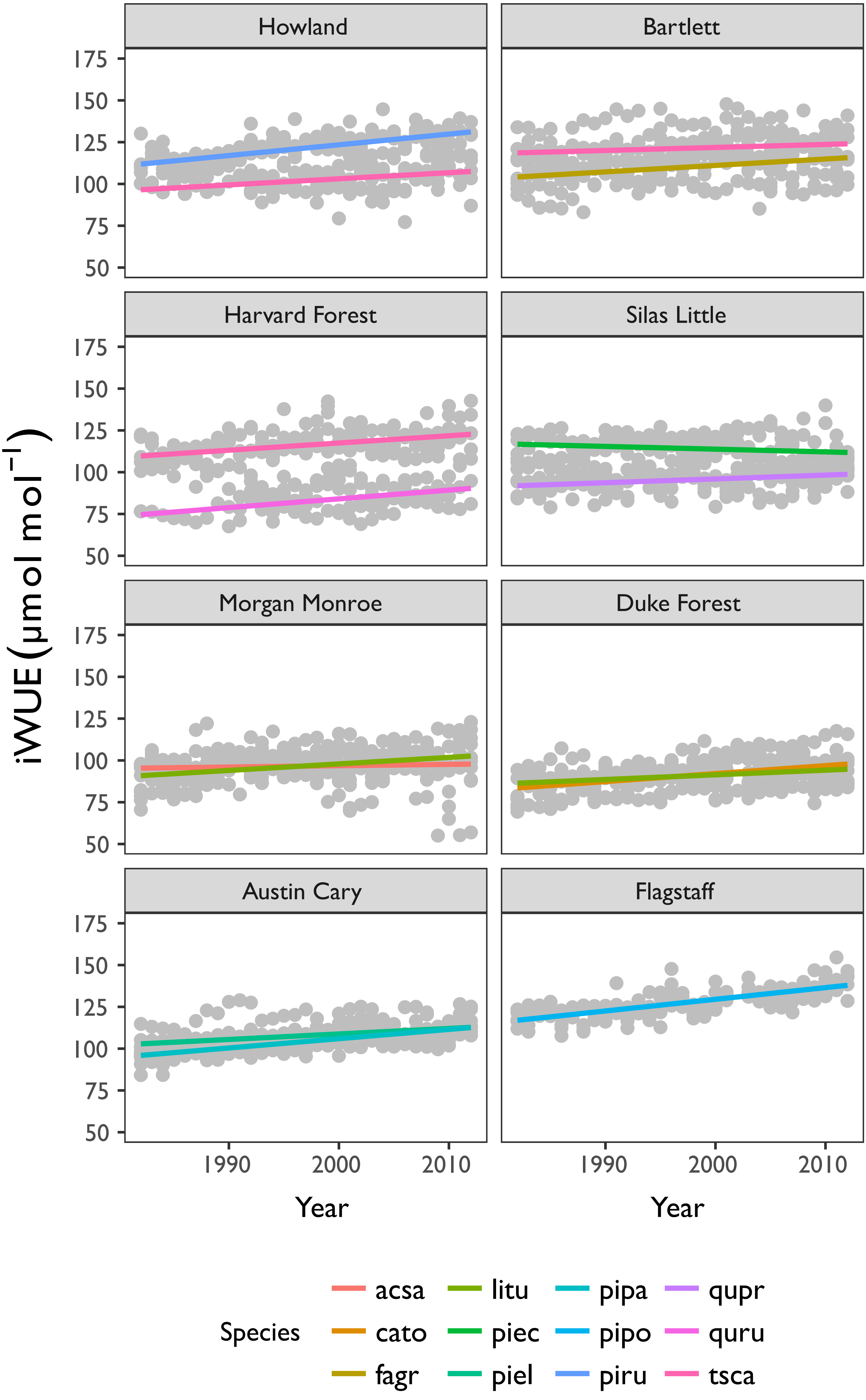

Howland
Bartlett
Harvard Forest
Silas Little
Morgan Monroe
Duke Forest
Austin Cary
Flagstaff
iWUE (μmol mol⁻¹)
175
150
125
100
75
50
1990
2000
2010
Year
Species
acsa
cato
fagr
litu
piec
piel
pipa
pipo
piru
qupr
quru
tsca

Figure S3 Change in iWUE observed in our study *vs.* previous studies in the literature. Percent changes in iWUE observed in our study (for the single species and all 8 sites together, red dots) under a 15% increase in atmospheric CO_2 concentration (c_a), in two global meta-analyses under a 17% (1960-2000 [14], indicated as 'global 47' in the y-axis; olive dot) and 26% (1950-2000 [15], indicated as 'global 53', green dot) increase in c_a, and in FACE experiments [16] (triangles; panel A). Boxplot of the ratio between relative changes in iWUE and c_a for all our observations under increase in 'ambient' c_a and for species at FACE experiments [16] (panel B).

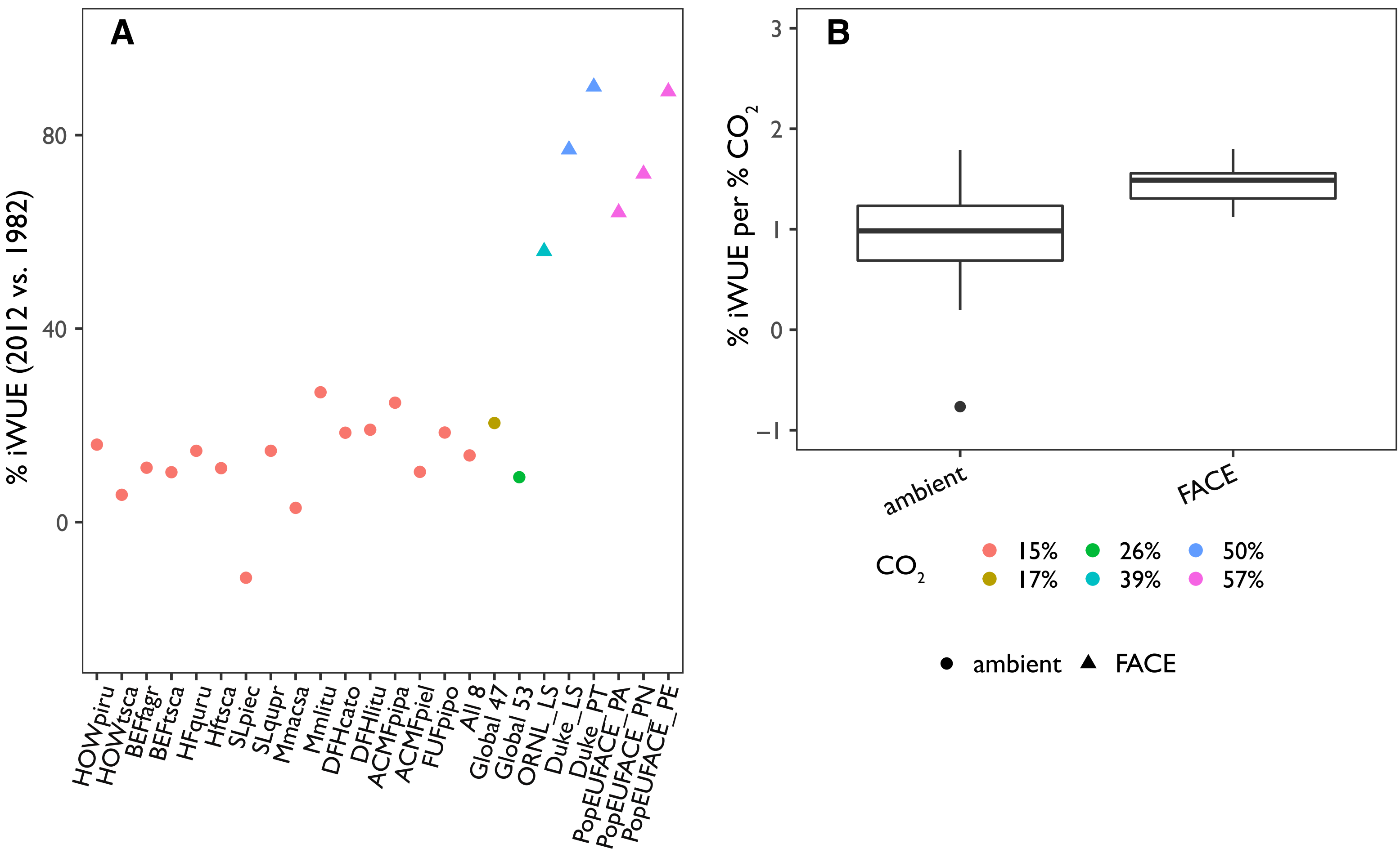

A
% iWUE (2012 vs. 1982)
80
40
0
HOWpiru
HOWtsca
BEFfagr
BEFtsca
HFquru
Hftsca
SLpiec
SLqupr
Mmacsa
Mmlitu
DFHcato
DFHlitu
ACMFpipa
ACMFpiel
FUFpipo
All 8
Global 47
Global 53
ORNL_LS
Duke_LS
Duke_PT
PopEUFACE_PA
PopEUFACE_PN
PopEUFACE_PE
B
% iWUE per % CO2
3
2
1
0
−1
ambient
FACE
CO2
15%
17%
26%
39%
50%
57%
ambient
FACE

Figure S4 Long-term change in the intercellular CO_2. Trends in the intercellular CO_2, c_i (ppm) for the 12 tree species at eight AmeriFlux sites. Each point represents the values obtained from alpha-cellulose $\delta^{13}C$ measured for the last 30-years from n=5 replicates per species at each of the investigated sites (for a total 75 chronologies). The full name of each species and site is provided in Table S1. Note that some species are present at more than one site (e.g., *Tsuga canadensis* and *Liriodendron tulipifera*).

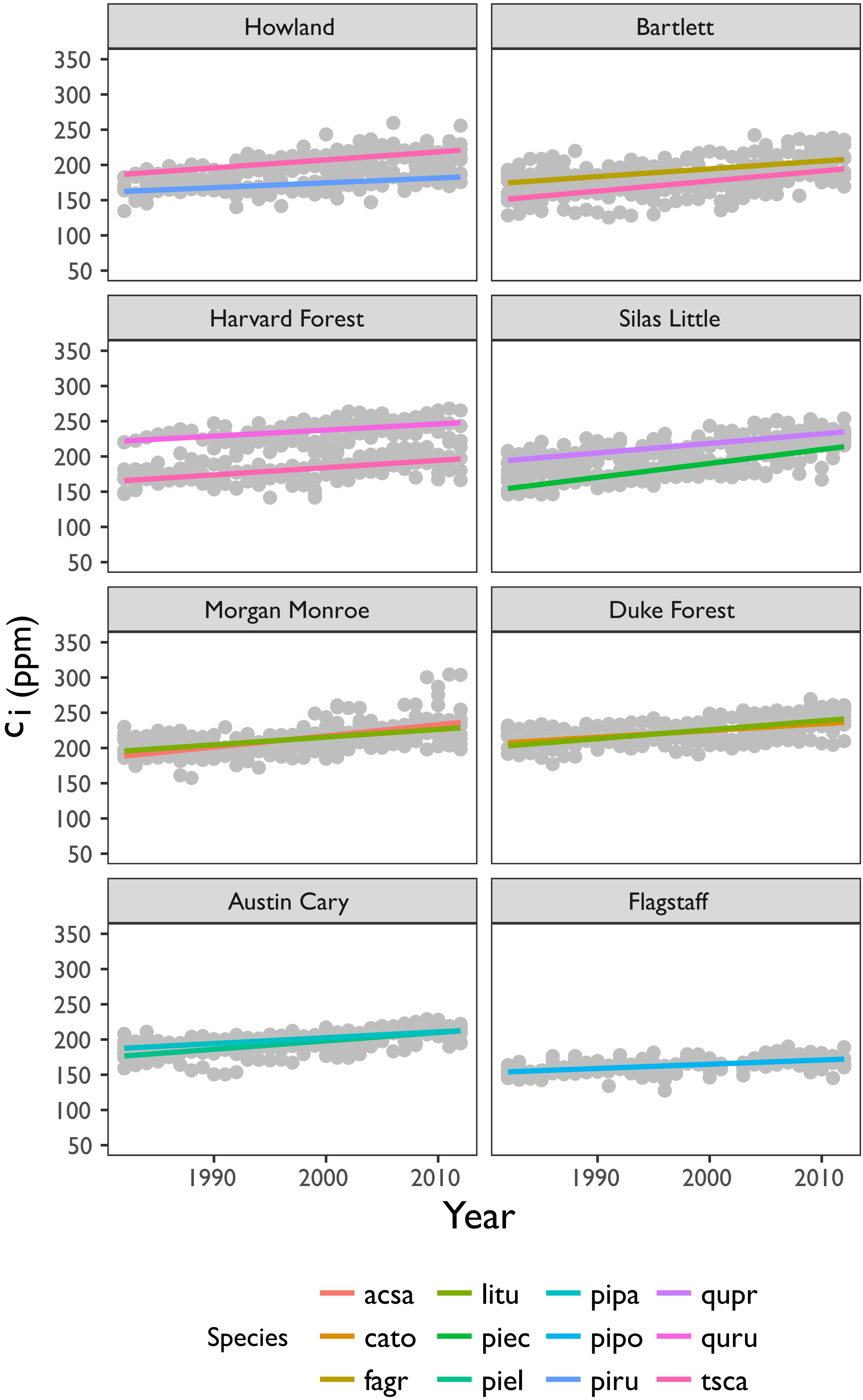

Howland
Bartlett
Harvard Forest
Silas Little
Morgan Monroe
Duke Forest
Austin Cary
Flagstaff
350
300
250
200
150
100
50
1990
2000
2010
c_i (ppm)
Year
Species
acsa
cato
fagr
litu
piec
piel
pipa
pipo
piru
qupr
quru
tsca

Figure S5 Long-term change in the ratio between intercellular CO_2 and atmospheric CO_2. Trends in the ratio between intercellular CO_2 and atmospheric CO_2 (c_i/c_a) across the 12 tree species (n=5 replicates per species for a total 75 chronologies) as calculated from tree-ring alpha-cellulose $\delta^{13}C$. Inset panel shows changes in c_i/c_a for the different species grouped by plant functional type (PFT) and wood anatomical features. Con, Diff-P and Ring-P indicate Coniferous, diffuse porous and ring porous species, respectively. The full name of each species is provided in Table S1.

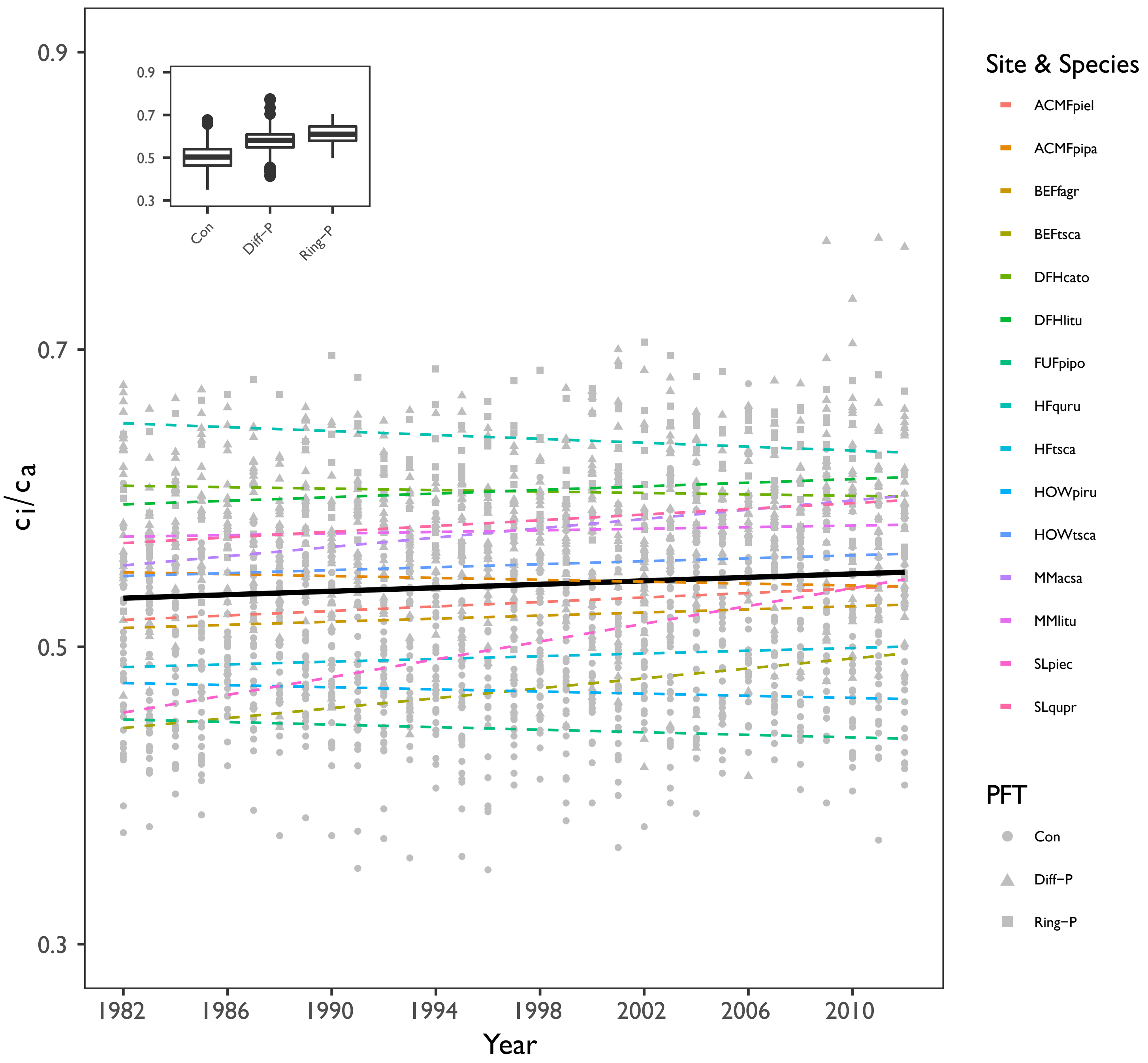

0.9
0.7
0.5
0.3
c_i/c_a
1982
1986
1990
1994
1998
2002
2006
2010
Year
Con
Diff−P
Ring−P
Site & Species
ACMFpiel
ACMFpipa
BEFfagr
BEFtsca
DFHcato
DFHlitu
FUFpipo
HFquru
HFtsca
HOWpiru
HOWtsca
MMacsa
MMlitu
SLpiec
SLqupr
PFT
Con
Diff−P
Ring−P

Figure S6 Long-term change in carbon isotope discrimination. Trends in carbon isotope discrimination, $\Delta^{13}C_c$ (‰ per year), as obtained from the tree-ring alpha-cellulose $\delta^{13}C_c$ measured for the 12 tree species at eight AmeriFlux sites. Each point represents the values calculated from $\delta^{13}C_c$ measured for the last 30-years from n=5 replicates per species at each of the investigated sites (for a total of 75 chronologies). Different symbols were used to indicate the three plant functional type (PFT): Coniferous (Con), diffuse porous (Diff-P) and ring porous (Ring-P) species. The full name of each species is provided in Table S1. Note that some species are present at more than one site (e.g., *Tsuga canadensis* and *Liriodendron tulipifera*).

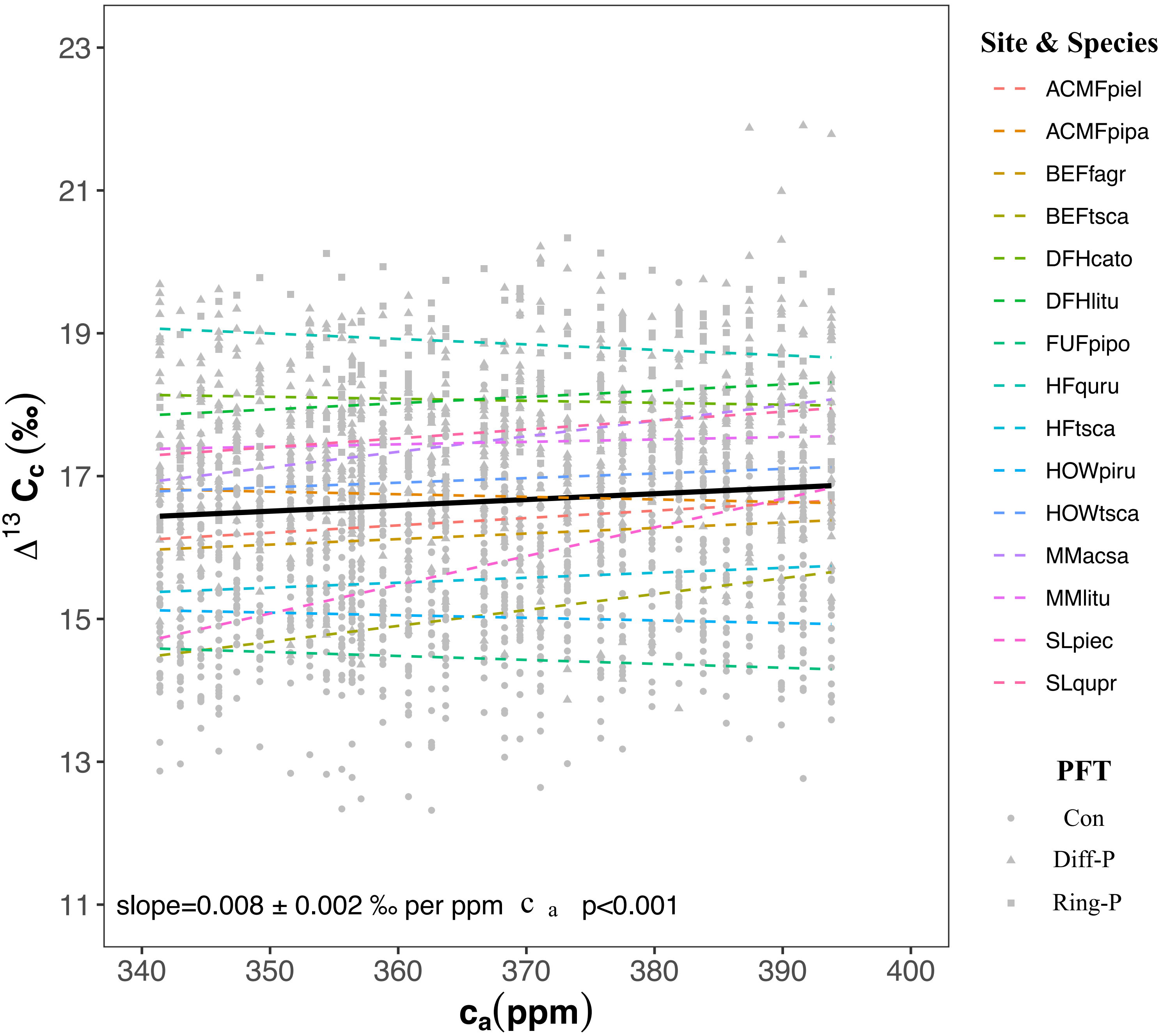

Site & Species
ACMFpiel
ACMFpipa
BEFfagr
BEFtsca
DFHcato
DFHlitu
FUFpipo
HFquru
HFtsca
HOWpiru
HOWtsca
MMacsa
MMlitu
SLpiec
SLqupr
PFT
Con
Diff-P
Ring-P
slope=0.008 ± 0.002 ‰ per ppm c a p<0.001
Δ13 Cc (‰)
ca(ppm)
23
21
19
17
15
13
11
340
350
360
370
380
390
400

Figure S7 Long-term change in basal area increment. Trends in basal area increment (BAI) measured for the 12 tree species at eight AmeriFlux sites. Each point represents the values calculated from ring widths measured for the last 30-years from n=5 replicates (2-3 wood cores per tree) per species at each of the investigated sites. The full name of each species is provided in Table S1. Slopes and standard error from the linear regression analyses are shown in the Figure 3A.

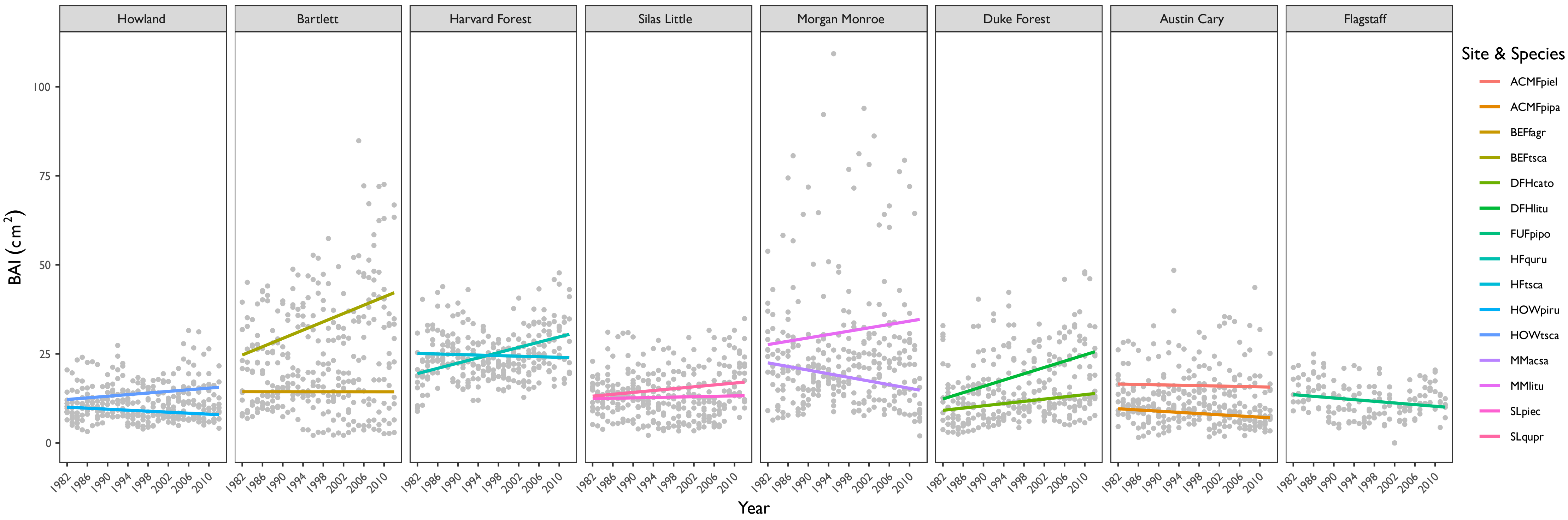
Howland
Bartlett
Harvard Forest
Silas Little
Morgan Monroe
Duke Forest
Austin Cary
Flagstaff
BAI (cm^2)
100
75
50
25
0
1982
1986
1990
1994
1998
2002
2006
2010
Year
Site & Species
ACMFpiel
ACMFpipa
BEFfagr
BEFtsca
DFHcato
DFHlitu
FUFpipo
HFquru
HFtsca
HOWpiru
HOWtsca
MMacsa
MMlitu
SLpiec
SLqupr

Figure S8 Changes in iWUE vs. BAI. Relationship between iWUE and BAI for each tree species (n=5 replicates per species) at the investigated AmeriFlux sites. We report slopes ± standard error only when significant positive (in black) or negative (in red) trends were observed. Stars indicate $p<0.05$ (*) and $p< 0.001$(***). The full name of sites and species is provided in Table S1. Our results are in line with previous studies in the literature reporting that increase in iWUE did not always correspond to an increase in BAI, see e.g., [17,14,18,19,20,21].

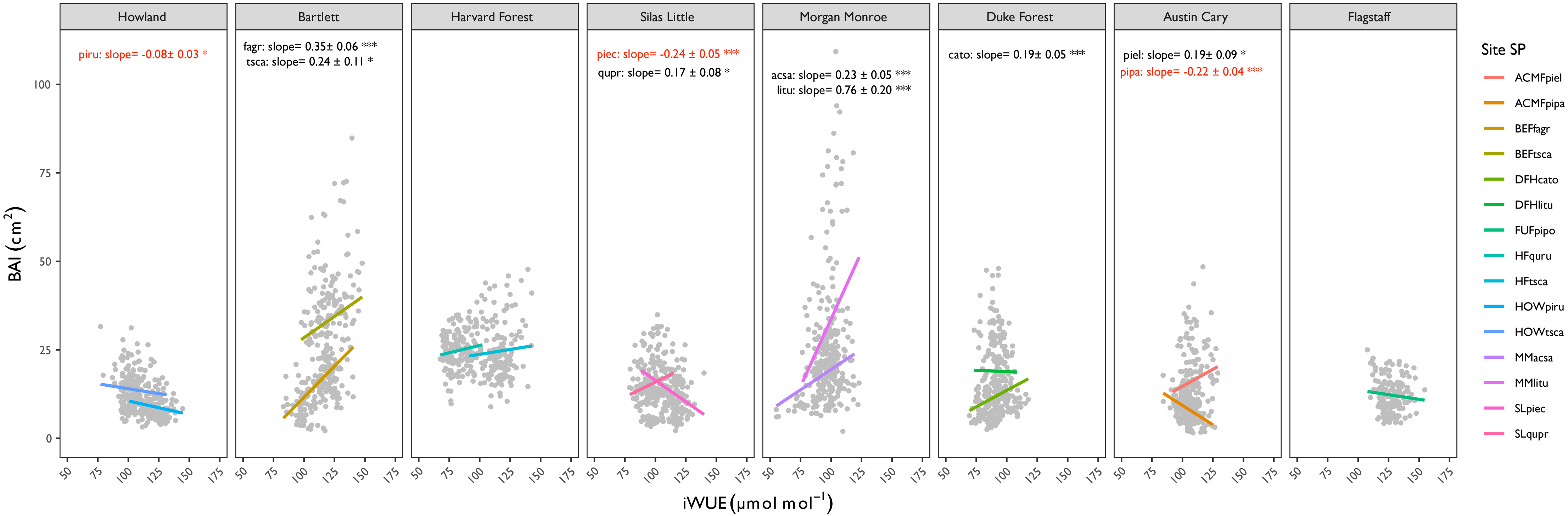
Howland
piru: slope= -0.08± 0.03 *
Bartlett
fagr: slope= 0.35± 0.06 ***
tsca: slope= 0.24 ± 0.11 *
Harvard Forest
Silas Little
piec: slope= -0.24 ± 0.05 ***
qupr: slope= 0.17 ± 0.08 *
Morgan Monroe
acsa: slope= 0.23 ± 0.05 ***
litu: slope= 0.76 ± 0.20 ***
Duke Forest
cato: slope= 0.19± 0.05 ***
Austin Cary
piel: slope= 0.19± 0.09 *
pipa: slope= -0.22 ± 0.04 ***
Flagstaff
BAI (cm^2)
iWUE (μmol mol^-1)
Site SP
ACMFpiel
ACMFpipa
BEFfagr
BEFtsca
DFHcato
DFHlitu
FUFpipo
HFquru
HFtsca
HOWpiru
HOWtsca
MMacsa
MMlitu
SLpiec
SLqupr

Figure S9 Comparison of measured and estimated $\delta^{18}O$ in soil and leaf water at two of the investigated sites. Panel A) compares estimated $\delta^{18}O$ in precipitation ($\delta^{18}O_P$) with measured $\delta^{18}O$ in soil water (in the first 10 cm of the soil) and stem water at Harvard and Austin Cary Memorial forests. The $\delta^{18}O$ in the soil water (i.e., the source water, $\delta^{18}O_{sw}$) reflects the $\delta^{18}O_P$, modified by evaporation processes. Because no isotope fractionation occurs during water uptake by root, stem water $\delta^{18}O$ accurately reflects the $\delta^{18}O$ of soil water taken up by trees [22]. Panel B) shows estimated *vs.* measured $\Delta^{18}O_{LW}$ values for two consecutive years. The Method in the legend refers to the estimate of $\Delta^{18}O_{LW}$ as derived from the alpha-cellulose $\delta^{18}O$ ($\Delta^{18}O_c$) and climate parameters (see Methods in the main text for details) and by using the steady-state Craig and Gordon model [2] (see Supplementary text). Each point represents the mean (± confidence interval) over number of replicates (n=3-4 days, when measurements were carried out for $\delta^{18}O$ in soil water; n=2 trees per 3-4 sampling days for measured $\delta^{18}O_{LW}$; n=5 trees for estimated $\Delta^{18}O_{LW}$ as described in the Methods) for 2004 and 2005.

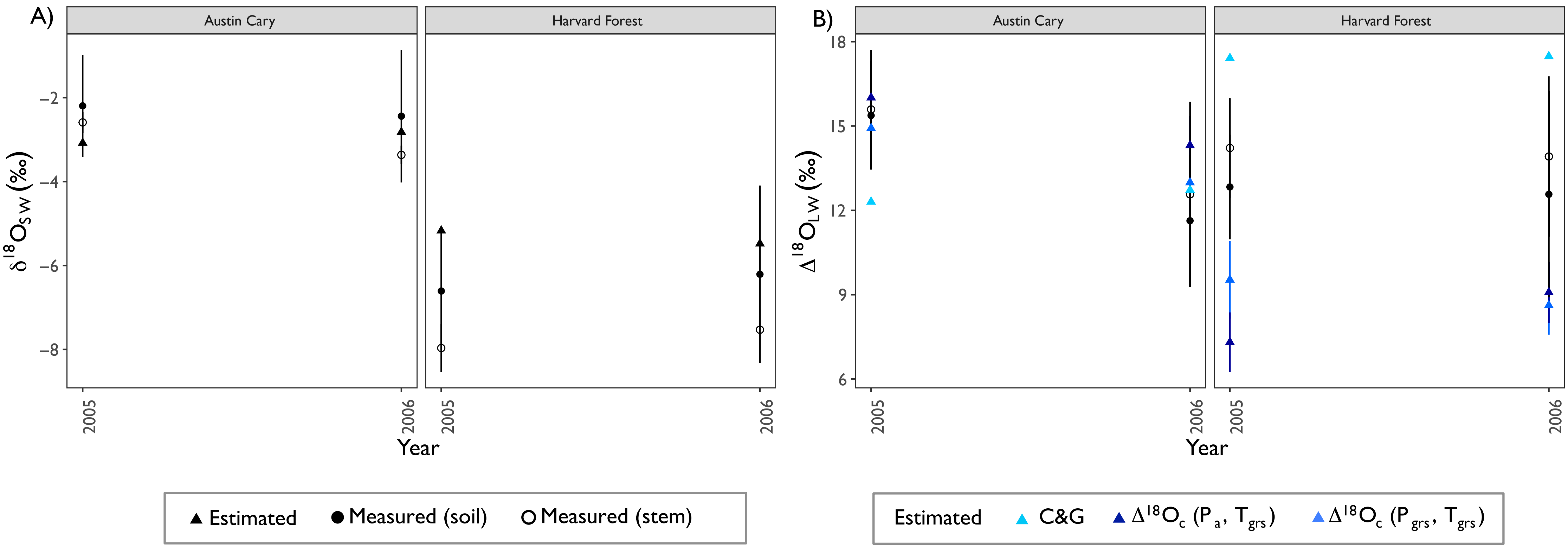

A)
Austin Cary
Harvard Forest
δ18OSW (‰)
−2
−4
−6
−8
2005
2006
Year
▲ Estimated
● Measured (soil)
○ Measured (stem)
B)
Austin Cary
Harvard Forest
Δ18OLW (‰)
18
15
12
9
6
2005
2006
Year
Estimated
C&G
Δ18Oc (Pa, Tgrs)
Δ18Oc (Pgrs, Tgrs)

Figure S10 Change in precipitation over the investigated years. Changes in growing season (mean over May-September months, P_{grs}) and annual precipitation (P_a) across the eight sites. Note that we only found a significant trend in the case of P_a at Bartlett (slope ± standard error = 0.92 ± 0.34 cm year^{-1}, $p<0.05$) and Flagstaff (slope ± standard error = -0.74 ± 0.26 cm year^{-1}, $p<0.01$).

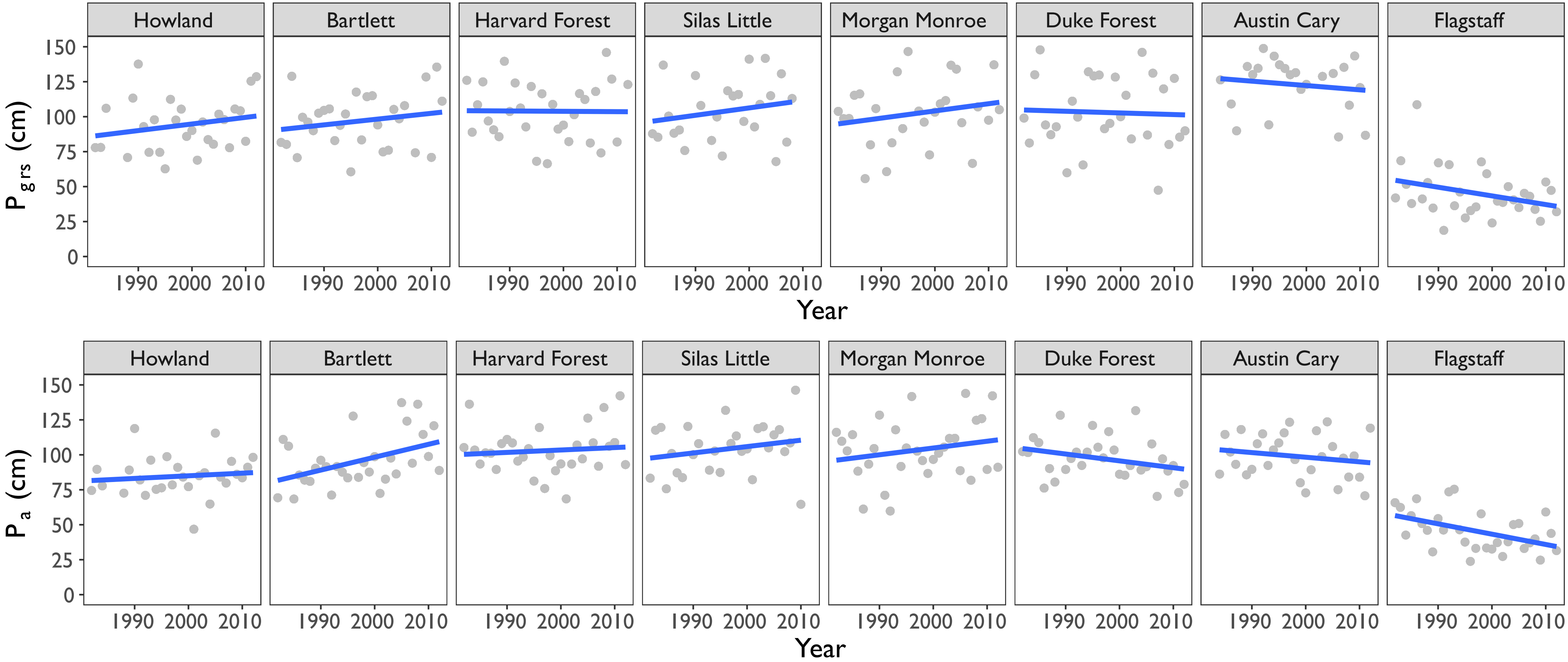

Howland
Bartlett
Harvard Forest
Silas Little
Morgan Monroe
Duke Forest
Austin Cary
Flagstaff
P_{grs} (cm)
Pa (cm)
Year

Figure S11 Change in vapour pressure deficit over the investigated years. Change in vapour pressure deficit, VPD, at the investigated sites as obtained from CRU dataset. Each point is the mean calculated over the May-September months, which is the same time window considered for flux data and other climate parameters. We found a significant increase in VPD for Austin Cary (slope ± standard error = 0.003 ± 0.001 kPa $year^{-1}$, $p<0.05$), Duke Forest (slope ± standard error = 0.008 ± 0.002 kPa $year^{-1}$, $p<0.001$), Flagstaff (slope ± standard error = 0.003 ± 0.001 kPa $year^{-1}$, $p<0.01$), Harvard forest (slope ± standard error = 0.003 ± 0.001 kPa $year^{-1}$, $p<0.05$) and Silas Little (slope ± standard error = 0.009 ± 0.002 kPa $year^{-1}$, $p<0.001$).

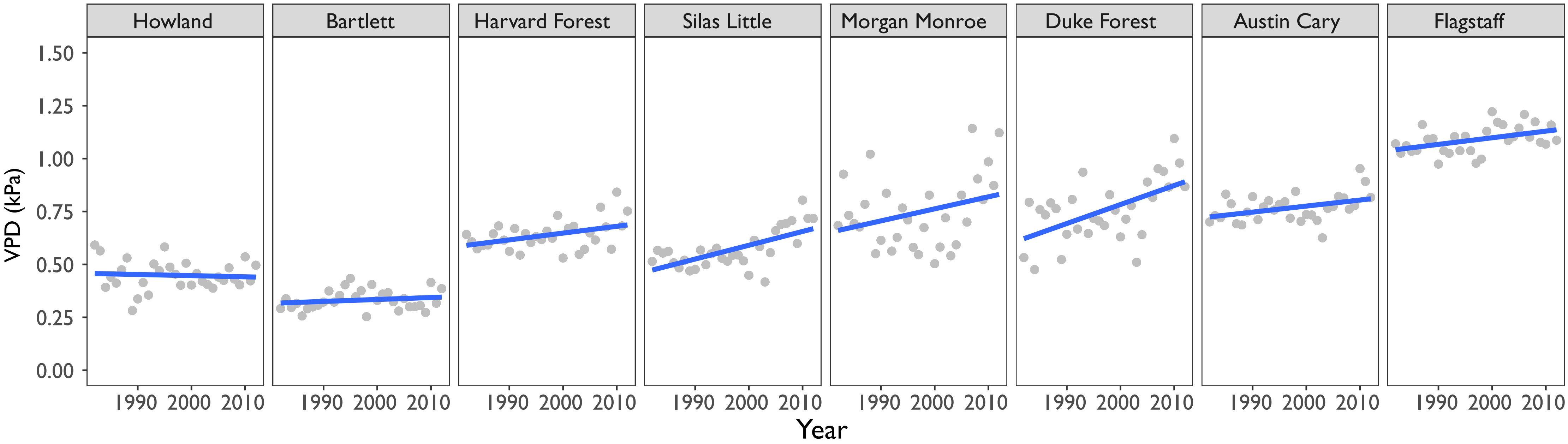
Howland
Bartlett
Harvard Forest
Silas Little
Morgan Monroe
Duke Forest
Austin Cary
Flagstaff
VPD (kPa)
1.50
1.25
1.00
0.75
0.50
0.25
0.00
1990
2000
2010
Year

Figure S12 Change in the standard precipitation-evaporation index over the investigated years. Change in standard precipitation-evaporation index relative to August with three months lag (SPEI8_3). We found a significant ($p<0.05$) increase in SPEI only at Bartlett, Howland, Morgan Monroe and Harvard forest ($p=0.08$).

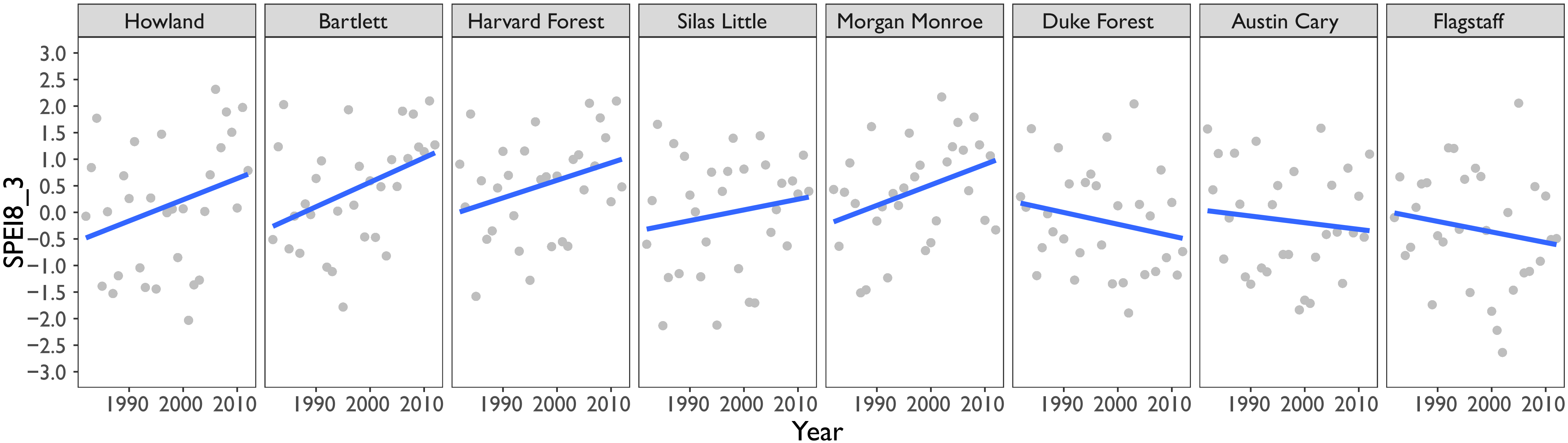
Howland
Bartlett
Harvard Forest
Silas Little
Morgan Monroe
Duke Forest
Austin Cary
Flagstaff
SPEI8_3
3.0
2.5
2.0
1.5
1.0
0.5
0.0
−0.5
−1.0
−1.5
−2.0
−2.5
−3.0
1990
2000
2010
Year

Figure S13 Relationship between intercellular and atmospheric CO_2 only for years where eddy covariance data were available. Change in c_i as obtained from the tree-ring alpha-cellulose $\delta^{13}C$ values relative to changes in atmospheric CO_2 (c_a). Each point represents the mean over the two dominant species at each site and for the years where eddy covariance data were available (SI Appendix, Table S1). We report slopes and standard error (in bracket) from linear regression at each site (indicated with different color lines) and with all sites together (black dashed line).

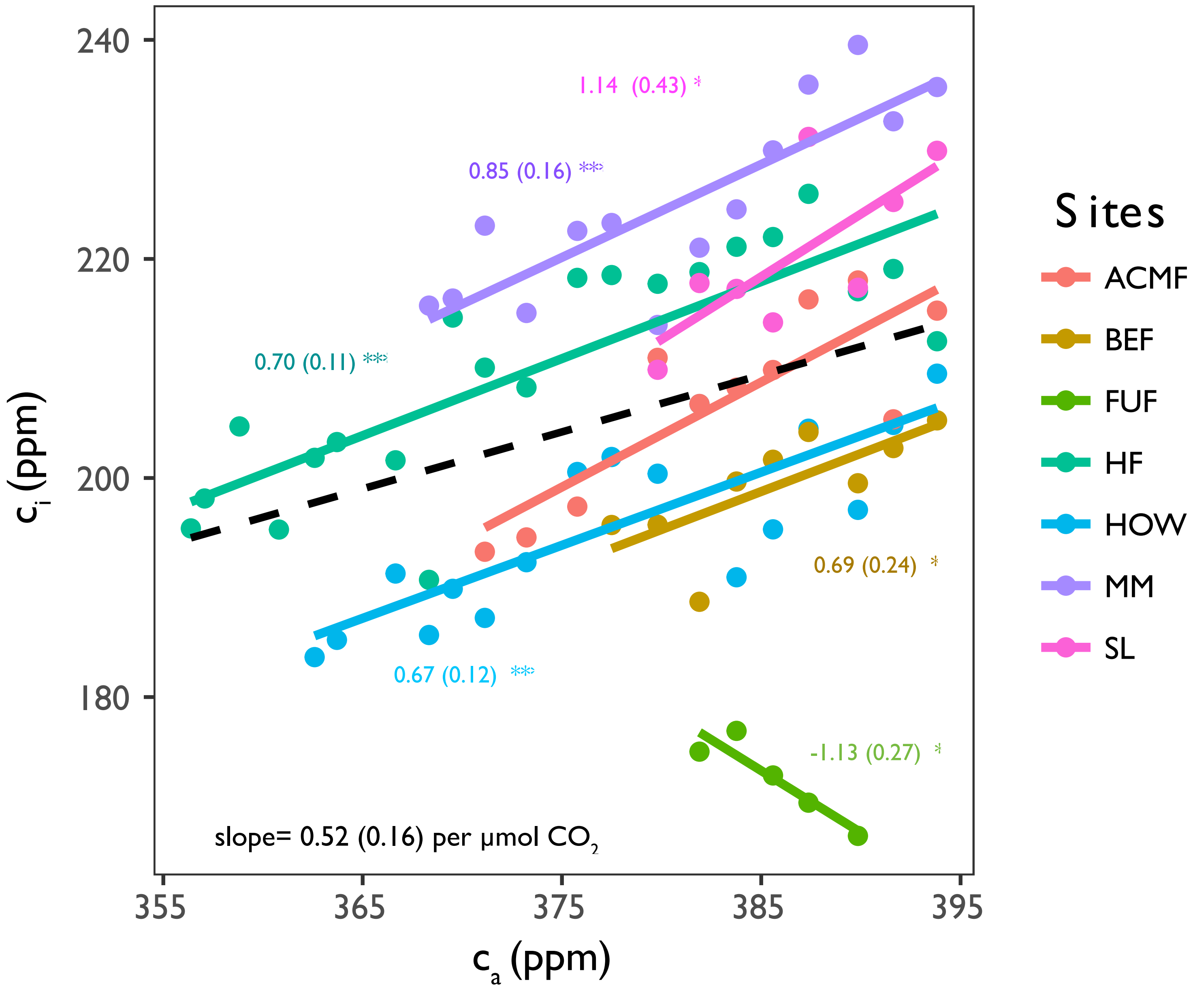

240
220
200
180
355
365
375
385
395
c_i (ppm)
c_a (ppm)
1.14 (0.43) *
0.85 (0.16) **
0.70 (0.11) **
0.67 (0.12) **
0.69 (0.24) *
-1.13 (0.27) *
slope= 0.52 (0.16) per µmol CO_2
Sites
ACMF
BEF
FUF
HF
HOW
MM
SL

Figure S14 Foliar nitrogen content across the investigated species. Foliar nitrogen content (% N) for each of the species at the investigated sites, as obtained from our previous study [23].

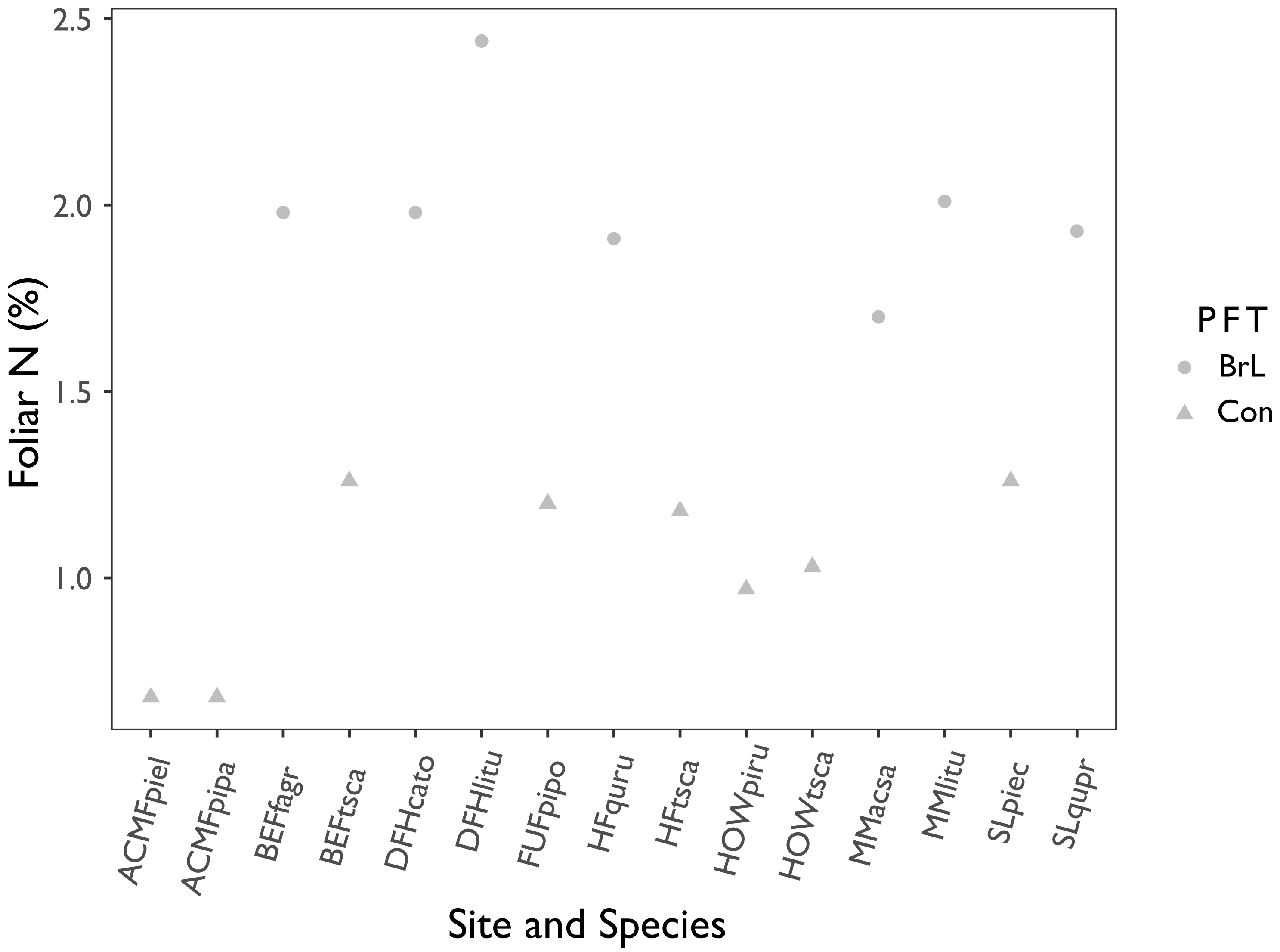

Foliar N (%)
2.5
2.0
1.5
1.0
PFT
BrL
Con
ACMFpiel
ACMFpipa
BEFfagr
BEFtsca
DFHcato
DFHlitu
FUFpipo
HFquru
HFtsca
HOWpiru
HOWtsca
MMacsa
MMlitu
SLpiec
SLqupr
Site and Species

Figure S15 Temporal changes in stomatal conductance (*g_s*) as predicted from the water-carbon optimality model. Trend in the annual mean (and site-level) g_s, weighted by daily GPP, as predicted by the carbon-water optimality model [24,25]. We present the output from different scenarios: no changes in c_a and climate (c0t0), changes in only climate (c0t1), changes in only c_a (c1t0) and changes in both c_a and climate (c1t1).

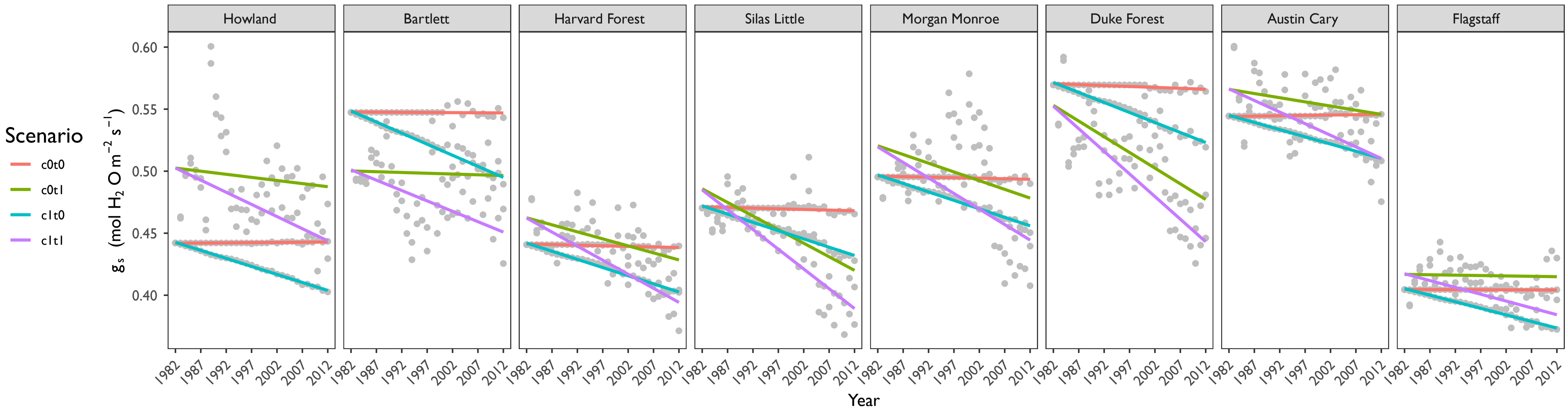
Scenario
c0t0
c0t1
c1t0
c1t1
g_s (mol H_2O m^{-2} s^{-1})
Howland
Bartlett
Harvard Forest
Silas Little
Morgan Monroe
Duke Forest
Austin Cary
Flagstaff
Year

Figure S16 Change in the leaf area index. Change in leaf area index (LAI) as obtained for each of the investigated sites from MODIS/Terra+Acqua 8-day with 500 m resolution as described in the SI Appendix. Each point represent the mean ± standard deviation over maximum values obtained through the growing season months (May-September). No significant trends in LAI were observed.

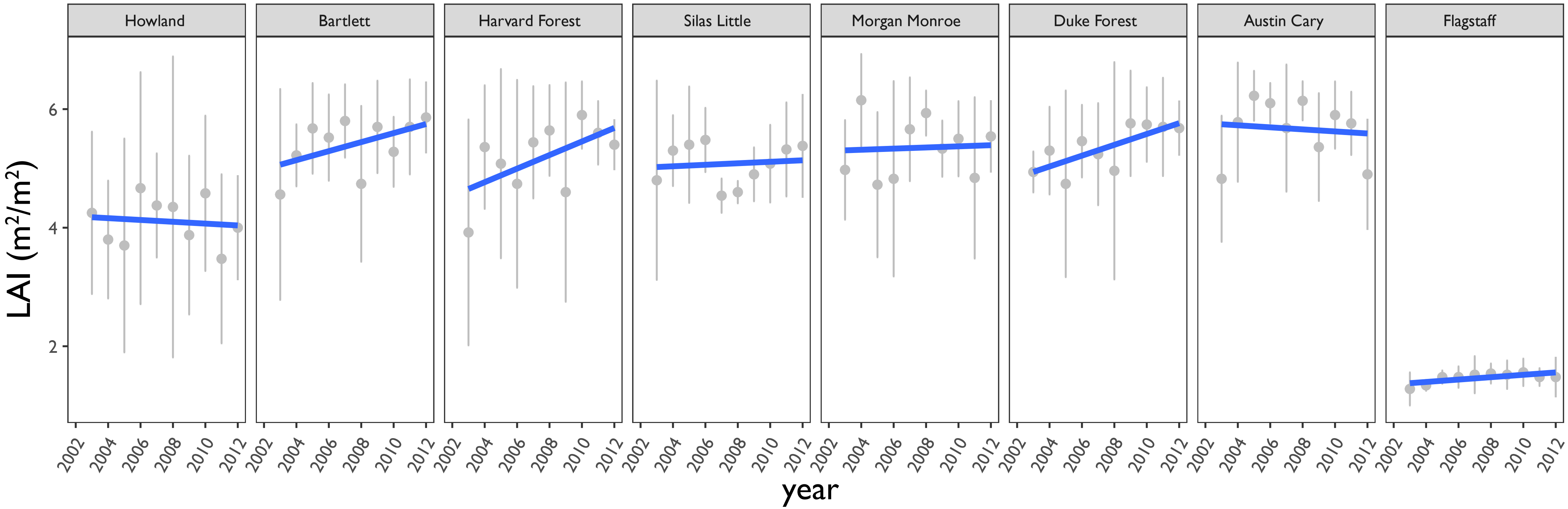

Howland
Bartlett
Harvard Forest
Silas Little
Morgan Monroe
Duke Forest
Austin Cary
Flagstaff
LAI (m²/m²)
6
4
2
2002
2004
2006
2008
2010
2012
year

Figure S17 Change in evapotranspiration at the investigated sites. Change in evapotranspiration (ET) as derived from eddy covariance flux measurements at 7 of the 8 sites included in the study. We did not observe significant trends in ET with the exception of Austin Cary, where ET increased. We cannot, however, exclude that ET estimate for this site is affected by the dense understory dominated by saw palmetto, which was shown to account for 25–35% of the above-canopy net CO_2 exchange [26].

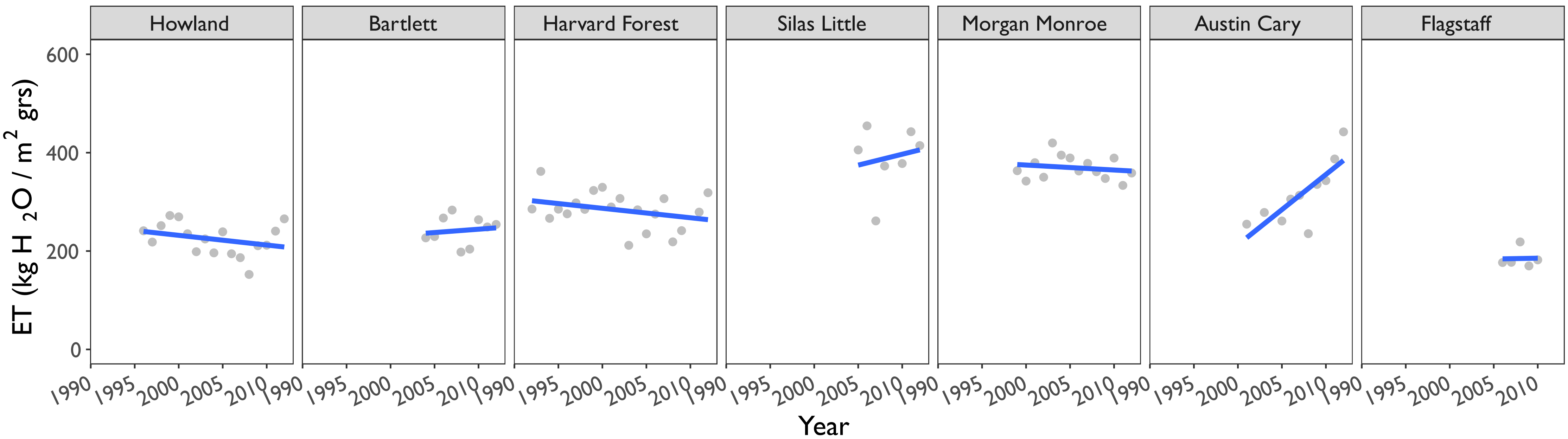

Howland
Bartlett
Harvard Forest
Silas Little
Morgan Monroe
Austin Cary
Flagstaff
ET (kg H 2O / m2 grs)
0
200
400
600
1990
1995
2000
2005
2010
Year

Figure S18 Change in $\delta^{18}O$ of precipitation at the investigated sites. Temporal changes in $\delta^{18}O$ in precipitation ($\delta^{18}O_P$) estimated at each of the investigated sites as described in the Supplementary text. No significant trends were detected.

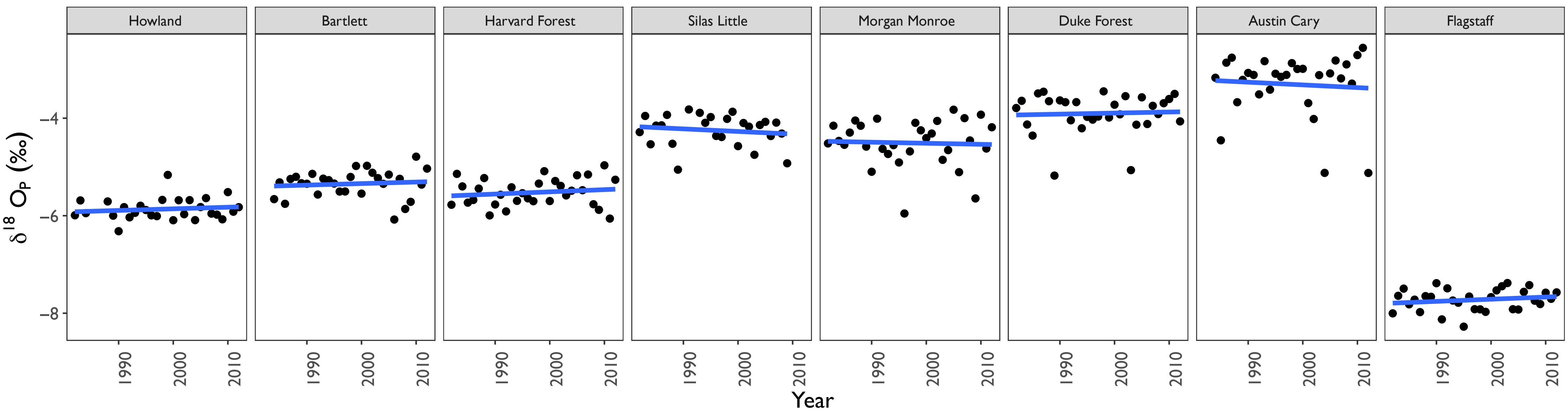

Howland
Bartlett
Harvard Forest
Silas Little
Morgan Monroe
Duke Forest
Austin Cary
Flagstaff
δ18 Op (‰)
−4
−6
−8
1990
2000
2010
Year

Figure S19 Change in relative humidty at the investigated sites. Temporal changes in relative humidity (RH) at each of the investigated sites as derived from growing season (May-September) VPD and temperature (gray dots). No significant changes were detected, with the exception of Duke (slope = -0.32 ± 0.09, p<0.001) and Silas Little (slope = -0.42 ± 0.16, p<0.05) forests, where we observed a reduction of RH. Blue dots indicate the RH as obtained from eddy covariance data (i.e., directly available as RH or back calculated from VPD and temperature). Mean over the growing season was calculated from half-hourly data, as described in the method.

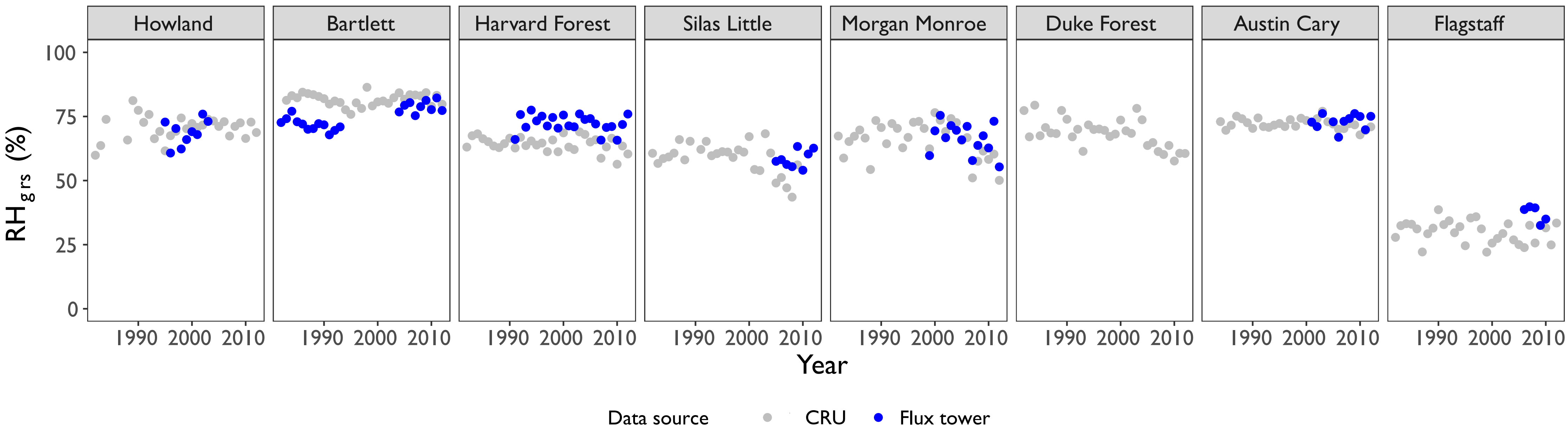
Howland
Bartlett
Harvard Forest
Silas Little
Morgan Monroe
Duke Forest
Austin Cary
Flagstaff
RH_grs (%)
100
75
50
25
0
1990
2000
2010
Year
Data source
CRU
Flux tower

Table S1. Description of the sites considered in this study. Age of the forest and Leaf Area Index (LAI) were obtained by the biological and ancillary data available online at the AmeriFlux network server. The fraction of each of the two dominant species included in the study was derived from a) camera-point quadrat measurements carried out in 6-12 plots around each flux tower, except for ACMF, which were based on basal area data and b) AmeriFlux biological data available for the investigated sites. Mesic and xeric sites were identified based on precipitation (P) changes for 1991-2012 compared to the 1901-1960 average, as obtained from the map showed in Figure 2.12 in ref 27. The last column reports the years we included for assessing ecosystem WUE based on eddy covariance measurements [23].

Site	AmeriFlux ID	Lat °N	Long °W	Elevation m *asl*	Forest type	Dominant species used for C and O isotope analyses	Fraction (%) (a)	(b)	Age (year)	LAI m^2m^{-2}	P changes (%)	Flux data (Years)
Austin Cary, FL (ACMF)	US-SP1	29°74'	82°22'	44	Pine flatwoods	*Pinus palustris* Mill. (pipa) *Pinus elliottii* Engelm (piel)	0.71 0.29	0.73 0.27	80	2.9	-5 to 0%	2001-2012 (2004 n/a)
Bartlett, NH (BEF)	US-Bar	44°06'	71°29'	272	Temperate Northern Hardwood	*Fagus grandifolia* Ehrh. (fagr) *Tsuga canadensis* (L.) Carr. (tsca)	0.34 0.36	0.21 0.21	99	4.5	10 to 15 %	2004-2012
Duke, NC (DFH)	US-Dk2	35°97'	79°10°	168	Southern hardwood	*Liriodendron tulipifera* L. (litu) *Carya tomentosa* L. (cato)	0.12 0.20	0.21 0.46	106	5.6	-5 to 0%	n/a
Flagstaff Unmanaged Forest, AZ (FUF)	US-Fuf	35°09'	111°76'	2180	Semi-arid Ponderosa pine	*Pinus ponderosa* Dougl. ex P. Laws. (pipo)		0.95	100	2.2	-10 to -5%	2006-2010
Harvard, MA (HF)	US-Ha1	42°54'	72°17'	340	Temperate deciduous	*Quercus rubra* L (quru) *Tsuga canadensis* (L.) Carr. (tsca)	0.41 0.34	0.36 0.13	80	4.9	10 to 15 %	1992-2012
Howland, ME (HOW)	US-Ho1	45°20'	68°74'	60	Transitional evergreen boreal	*Picea rubens* Sarg. (piru) *Tsuga canadensis* (L.) Carr. (tsca)	0.82 0.16	0.41 0.29	109	5.7	5 to 10 %	1996-2012
Morgan Monroe, IN (MM)	US-MMS	39°32'	86°41'	275	Mixed temperate Deciduous	*Acer saccharum* Marsh. (acsa) *Liriodendron tulipifera* L. (litu)	0.17 0.17	0.17 0.17	70	4.9	10 to 15 %	1999-2012
Silas Little, NJ (SL)	US-Slt	39°91'	74°60'	30	Mixed Pineland	*Quercus prinus* L. (qupr) *Pinus echinata* Mill. (piec)	0.25 0.55	0.25 0.11	100	4.8	0 to 5 %	2005-2012

Table S2. Linear mixed-effects model for iWUE. Results from the linear mixed effects model (LME) for iWUE where plant functional types (LME^1) or wood anatomical features (LME^2), together with atmospheric CO_2 (c_a) and environmental parameters were included as fixed factors. We considered random intercept for Tree IDs nested in Species and nested in Site. R^2 marginal and R^2 conditional indicate the variance explained by only fixed factors and fixed + random factors, respectively. Environmental parameters included in the model were: growing season (through May-September) temperature and precipitation (T_{grs} and P_{grs}, respectively), the standard precipitation-evaporation index, SPEI, relative to August, with 3 months' lag (SPEI8_3), atmospheric CO_2 (c_a, mean over summer months as for T_{grs} and P_{grs}) and growing season vapour pressure deficit (VPD_{grs}). Estimate represents the value of Intercept and coefficients of predictor variables (for each of the fixed factor), while SE indicates the standard error.

Fixed effects		Estimate ± SE	p-value	R^2 marginal	R^2 conditional
LME^1	Intercept	94.12±2.84	<0.001	0.48	0.83
	Conifer vs. Deciduous	21.79± 2.58	<0.001		
	P_{grs}	-0.02 ±0.005	<0.001		
	T_{grs}	0.48±0.21	<0.05		
	SPEI8_3	-0.53±0.13	<0.001		
	c_a	0.20±0.015	<0.001		
	VPD_{grs}	3.81±1.73	<0.05		
LME^2	Intercept	114.64±2.77	<0.001	0.47	0.70
	Conifer vs. diffuse porous deciduous	17.80± 4.47	<0.01		
	Conifer vs. ring porous deciduous	26.04 ±6.21	<0.01		
	P_{grs}	-0.19±0.004	<0.001		
	T_{grs}	0.34±0.21	n.s.		
	SPEI8_3	-0.54±0.13	<0.001		
	c_a	0.20±0.017	<0.001		
	VPD_{grs}	5.98±1.79	<0.001		

Table S3. Results from linear regression analyses on iWUE for the investigated tree species. Slopes and standard error (SE) from the linear regression analyses on iWUE for each species at the investigated AmeriFlux sites. Stars indicate slopes that were significantly different from zero with (*) $p<0.05$, (**) $p<0.01$, (***) $p<0.001$, while n.s. indicates slope no significantly different from zero.

Site	**Species**	**iWUE (µmol/mol per year)**		
		Slope	SE	**p-value**
Austin Cary	piel	0.33	0.14	***
	pipa	0.56	0.47	***
Bartlett	fagr	0.39	0.08	***
	tsca	0.18	0.02	n.s.
Duke forest	cato	0.48	0.16	***
	litu	0.28	0.12	***
Flagstaff	pipo	0.7	0.52	***
Harvard forest	quru	0.52	0.30	***
	tsca	0.43	0.16	***
Howland	piru	0.64	0.44	***
	tsca	0.36	0.17	***
Morgan Monroe	acsa	0.08	0.003	n.s.
	litu	0.39	0.19	***
Silas Little	piec	-0.16	0.03	*
	qupr	0.23	0.08	***

Table S4. Linear mixed-effects model for c_i Results from the linear mixed effects model for c_i where c_a and plant functional types (LME^1), or wood anatomical features (LME^2), or environmental parameters (LME^3) were included as fixed factors. We considered random intercept and Tree IDs nested in Species and nested in Site. R^2 marginal and R^2 conditional indicate the variance explained by only fixed factors and fixed + random factors, respectively. Environmental parameters included in the model were: growing season (through May-September) temperature and precipitation (T_{grs} and P_{grs}, respectively), the standard precipitation-evaporation index, SPEI, relative to August, with 3 months' lag (SPEI8_3), atmospheric CO_2 (c_a, mean over summer months as for T_{grs} and P_{grs}) and growing season vapour pressure deficit (VPD_{grs}). Estimate represents the value of Intercept and coefficients of predictor variables (for each of the fixed factor), while SE indicates the standard error.

Fixed effects		Estimate ± SE	p-value	R^2 marginal	R^2 conditional
LME^1	Intercept	216.16±4.55	<0.001	0.51	0.84
	Conifer vs. Deciduous	-34.09±4.08	<0.001		
	c_a	0.67±0.022	<0.001		
LME^2	Intercept	184.27±4.48	<0.001	0.48	0.83
	Conifer vs. diffuse porous deciduous	-24.07±5.82	<0.001		
	Conifer vs. ring porous deciduous	-41.53±5.05	<0.001		
	c_a	0.67±0.022	<0.001		
LME^3	Intercept	216.37±4.555	<0.001	0.52	0.85
	Conifer vs. Deciduous	-34.87±4.127	<0.001		
	P_{grs}	0.03±0.008	<0.001		
	T_{grs}	-0.74±0.327	<0.05		
	SPEI8_3	0.86±0.207	<0.001		
	c_a,	0.67±0.024	<0.001		
	VPD_{grs}	-5.97±2.76	<0.05		

Table S5. Linear mixed-effects model for c_i/c_a. Results from the linear mixed effects model (LME) for the c_i/c_a ratio over time when only year (LME^1), plant functional types (LME^2) or wood anatomical features (LME^3) were included as fixed factors. We considered random intercept and Tree IDs nested in Species and nested in Site. R^2 marginal and R^2 conditional indicate the variance explained by only fixed factors and fixed + random factors, respectively. Estimate represents the value of Intercept and coefficients of predictor variables (for each of the fixed factor), while SE indicates the standard error.

Fixed effects		Estimate ± SE	p-value	R^2 marginal	R^2 conditional
LME^1	Intercept	0.536±0.0163	<0.001	0.005	0.814
	Year	0.0005±0.0001	<0.001		
LME^2	Intercept	0.589±0.123	<0.001	0.446	0.817
	Conifer vs. deciduous	-0.093±0.011	<0.001		
	Year	0.0005±0.0001	<0.001		
LME^3	Intercept	0.501±0.012	<0.001	0.402	0.799
	Conifer vs. diffuse porous deciduous	-0.065±0.015	<0.001		
	Conifer vs. ring porous deciduous	-0.114±0.013	<0.001		
	Year	0.0005±0.0010	<0.001		

Table S6. Linear mixed-effects model for $\Delta^{13}C_c$. Results from the linear mixed effects model (LME) for $\Delta^{13}C_c$, where c_a and plant functional types (LME[1]) or wood anatomical features (LME[2]), or environmental parameters (LME[3]) were included as fixed factors. We considered random intercept and Tree IDs nested in Species and nested in Site. R^2 marginal and R^2 conditional indicate the variance explained by only fixed factors and fixed + random factors, respectively. Environmental parameters included in the model were: growing season (through May-September) temperature and precipitation (T_{grs} and P_{grs}, respectively), the standard precipitation-evaporation index, SPEI, relative to August, with 3 months' lag (SPEI8_3), atmospheric CO_2 (c_a, mean over summer months as for T_{grs} and P_{grs}) and growing season vapour pressure deficit (VPD_{grs}). Estimate represents the value of Intercept and coefficients of predictor variables (for each of the fixed factor), while SE indicates the standard error.

Fixed effects		Estimate ± SE	p-value	R^2 marginal	R^2 conditional
LME[1]	Intercept	17.71±0.28	<0.001	0.45	0.82
	Conifer vs. Deciduous	-2.11± 0.25	<0.001		
	c_a,	0.008±0.0013	<0.001		
LME[2]	Intercept	15.740 ±0.267	<0.001	0.40	0.80
	Conifer vs. diffuse porous deciduous	-1.483±0.358	<0.001		
	Conifer vs. ring porous deciduous	-2.574±0.310	<0.001		
	c_a,	0.008±0.0013	<0.001		
LME[3]	Intercept	17.72±0.28	<0.001	0.46	0.83
	Conifer vs. Deciduous	-2.16±0.25	<0.001		
	P_{grs}	0.002±0.0004	<0.001		
	T_{grs}	-0.039±0.02	<0.05		
	SPEI8_3	0.052±0.013	<0.001		
	c_a,	0.008±0.0015	<0.001		
	VPD_{grs}	-0.445±0.170	<0.01		

Table S7. Results from the linear regression analyses on modelled $\Delta^{18}O_{LW}$ values. Slopes from the linear regression analyses on $\Delta^{18}O_{LW}$ as obtained from equation 6 in the Methods, by estimating p_xp_{ex} from growing season precipitation (P_{grs}), annual precipitation (P_a) and by considering a fix p_xp_{ex} value of 0.4 (i.e., $p_x = 1$ and $p_{ex}=0.4$, [3]). Stars indicate slopes that were significantly different from zero with (*) $p<0.05$, (**) $p<0.01$, (***) $p<0.001$, while n.s. indicates slope no significantly different from zero.

Site	**Species**	**$p_xp_{ex} - P_{grs}$**		**$p_xp_{ex} - P_a$**		**Fix p_xp_{ex}**	
		Slope		*Slope*		*Slope*	
Austin Cary	piel	0.03	n.s.	0.07	***	0.05	**
	pipa	0.04	*	0.08	***	0.06	**
Bartlett	fagr	-0.09	***	-0.11	***	-0.06	***
	tsca	-0.05	*	-0.06	***	0.002	n.s.
Duke forest	cato	0.02	n.s.	0.04	**	0.006	n.s.
	litu	0.03	n.s.	0.05	**	0.02	n.s.
Flagstaff	pipo	0.25	***	0.31	***	0.08	***
Harvard forest	quru	-0.002	n.s.	0.007	n.s.	0.01	n.s.
	tsca	-0.003	n.s.	-0.02	n.s.	-0.01	n.s.
Howland	piru	-0.06	**	-0.05	*	-0.04	*
	tsca	-0.04	*	-0.02	n.s.	-0.009	n.s.
Morgan Monroe	acsa	-0.04	*	-0.02	n.s.	0.006	n.s.
	litu	-0.04	*	-0.02	n.s.	-0.001	n.s.
Silas Little	piec	-0.04	n.s.	-0.04	*	0.01	n.s.
	qupr	-0.09	***	-0.09	***	-0.06	***

Table S8. Full reference and link to access eddy covariance data for the AmeriFlux sites included in this study.

Site	AmeriFlux ID	Citation	Link
ACMF	US-SP1	Tim Martin AmeriFlux US-SP1 Slashpine-Austin Cary- 65yrs nat regen, doi:10.17190/AMF/1246100	http://dx.doi.org/10.17190/AMF/1246100
BEF	US-Bar	Andrew Richardson AmeriFlux US-Bar Bartlett Experimental Forest, doi:10.17190/AMF/1246030	http://dx.doi.org/10.17190/AMF/1246030
FUF	US-Fuf	Sabina Dore, Thomas Kolb AmeriFlux US-Fuf Flagstaff - Unmanaged Forest, doi:10.17190/AMF/1246051	http://dx.doi.org/10.17190/AMF/1246051
HF	US-Ha1	J. William Munger AmeriFlux US-Ha1 Harvard Forest EMS Tower (HFR1), doi:10.17190/AMF/1246059	http://dx.doi.org/10.17190/AMF/1246059
HOW	US-Ho1	David Hollinger AmeriFlux US-Ho1 Howland Forest (main tower), doi:10.17190/AMF/1246061	http://dx.doi.org/10.17190/AMF/1246061
MM	US-MMS	Kim Novick, Rich Phillips AmeriFlux US-MMS Morgan Monroe State Forest, doi:10.17190/AMF/1246080	http://dx.doi.org/10.17190/AMF/1246080
SL	US-Slt	Ken Clark AmeriFlux US-Slt Silas Little- New Jersey, doi:10.17190/AMF/1246096	http://dx.doi.org/10.17190/AMF/1246096

References

[1] Barbour MM, Andrews TJ, Farquhar GD (2001) Correlations between oxygen isotope ratios of wood constituents of Quercus and Pinus samples from around the world. *Australian Journal of plant physiology* 28: 335-348.

[2] Craig H, Gordon LI (1965) Deuterium and oxygen-18 variations in the ocean and the marine atmosphere. In Proceedings of a Conference on Stable Isotopes in Oceanographic Studies and Palaeotemperatures (ed E. Tongiorgi), pp. 9–130. Lischi and Figli, Pisa.

[3] Barbour MM (2007) Stable oxygen isotope composition of plant tissue: a review. *Functional Plant Biology* 34: 83–94.

[4] Farquhar GD, Cernusak LA, Barnes B (2007) Heavy water fractionation during transpiration. *Plant Physiology* 143: 11–18.

[5] Majoube M (1971). Fractionnement en oxygen-18 et en deuterium entre l'eau et sa vapeur. *Journal de Chimie et Physique 68*: 1423–1436.

[6] Cernusak LA, et al. (2016) Stable isotopes in leaf water of terrestrial plants. *Plant, Cell & Environment* 39: 1087-1102.

[7] Kahmen A, et al. (2008) Effects of environmental parameters, leaf physiological properties and leaf water relations on leaf water $\delta^{18}O$ enrichment in different Eucalyptus species. *Plant Cell Environment* 31(6): 738-51.

[8] Warren CR (2006) Stand aside stomata, another actor deserves centre stage: the forgotten role of the internal conductance to CO_2 transfer. *Journal of Experimental Botany* 59 (7): 475–1487.

[9] Guerrieri R, K Jennings, Belmecheri S, Asbjornsen H, Ollinger S (2017). Evaluating climate signal recorded in tree-ring $\delta^{13}C$ and $\delta^{18}O$ values from bulk wood and α-cellulose for six species across four sites in the northeastern US. *Rapid Commun Mass Spectrom.* 31:2081–2091.

[10] Myneni R, Knyazikhin, Y, Park T (2015) MOD15A2H MODIS/Terra Leaf Area Index/FPAR 8-Day L4 Global 500m SIN Grid V006 [Data set]. NASA EOSDIS Land Processes DAAC. doi: 10.5067/MODIS/MOD15A2H.006.

[11] Belmecheri S, et al. (2014) Tree-ring $\delta^{13}C$ tracks flux tower ecosystem productivity estimates in a NE temperate forest. *Environmental Research Letters* 9 (7): 074011.

[12] Jennings K, Guerrieri R, Vadeboncoeur MA, Asbjornsen H (2016) Response of *Quercus velutina* growth and water use efficiency to climate variability and nitrogen fertilization in a temperate deciduous forest in the northeastern USA *Tree Physiology* 36 (4): 428-43.

[13] Song X, Clark KS, Helliker BR (2014) Interpreting species-specific variation in tree-ring oxygen isotope ratios among three temperate forest trees *Plant Cell Environment* 37 (9): 2169-2182.

[14] Peñuelas J, Canadell JG, Ogaya R (2011) Increased water-use efficiency during the 20th century did not translate into enhanced tree growth. *Global Ecology and Biogeography* 20: 597-608.

[15] Leonardi S, et al. (2012) Assessing the effects of nitrogen deposition and climate on carbon isotope discrimination and intrinsic water-use efficiency of angiosperm and conifer trees under rising CO_2 conditions. *Global Change Biology* 18: 2925–2944.

[16] Battipaglia G, et al. (2013) Elevated CO_2 increases tree-level intrinsic water use efficiency: insights from carbon and oxygen isotope analyses in tree rings across three forest FACE sites. *New Phytologist* 197:544-554.

[17] Peñuelas J, Hunt JM, Ogaya R, Jump AS (2008). Twentieth century changes of tree-ring $\delta^{13}C$ at the southern range-edge of Fagus sylvatica: increasing water-use efficiency does not avoid the growth decline induced by warming at low altitudes. *Global Change Biology* 14: 1076–1088.

[18] van der Sleen P, Groenendijk P, Vlam M, Anten NPR, Boom A, Bongers F, Pons TL, Terburg G, Zuidema PA (2015). No growth stimulation of tropical trees by 150 years of CO_2 fertilization but water-use efficiency increased. *Nature Geoscience* 8: 24-28.

[19] Levesque M, Andreu-Hayles L, Pederson, N. (2017). Water availability drives gas exchange and growth of trees in northeastern US, not elevated CO_2 and reduced acid deposition. *Scientific Reports* 7: 46158.

[20] Martínez-Sancho E, Dorado-Liñán I, Gutiérrez-Merino E, Matiu M, Helle G, Heinrich I, Menzel A (2018). Increased water-use efficiency translates into contrasting growth patterns of Scots pine and sessile oak at their southern distribution limits. *Global Change Biology*, 24: 1012-2028.

[21] Reed CC, Ballantyne AP, Cooper LA, Sala A (2018). Limited evidence for CO_2-related growth enhancement in northern Rocky Mountain lodgepole pine populations across climate gradients. *Global Change Biology*, 24: 3922– 3937.

[22] Gessler A, et al. (2014) Stable isotopes in tree rings: towards a mechanistic understanding of isotope fractionation and mixing processes from the leaves to the wood. *Tree Physiology* 34 (8): 796–818.

[23] Guerrieri R, Lepine L, Asbjornsen H, Xiao J, Ollinger SV (2016) Evapotranspiration and water use efficiency in relation to climate and canopy nitrogen in U.S. forests. *Journal of Geophysical Research: Biogeosciences* 121: 2610–2629.

[24] Prentice C, Dong N, Gleason SM, Maire V, Wright IJ (2014) Balancing the costs of carbon gain and water transport: testing a new theoretical framework for plant functional ecology. *Ecology Letters* 17: 82–91.

[25] Wang H, et al. (2017) Towards a universal model for carbon dioxide uptake by plants. *Nature Plants* 3: 734-741.

[26] Powell TL, et al. (2008) Carbon exchange of a mature, naturally regenerated pine forest in north Florida. *Global Change Biology* 14: 2523–2538.

[27] Melillo JM, Richmond T, Gary WY (2014) Climate Change Impacts in the United States: The Third National Climate Assessment. U.S. Global Change Research Program, 841 pp.